UNIVERSITY *of* York

This is a repository copy of *Testing microscopically derived descriptions of nuclear collectivity:Coulomb excitation of 22Mg*.

White Rose Research Online URL for this paper:
https://eprints.whiterose.ac.uk/132362/

Version: Accepted Version

White Rose
university consortium
Universities of Leeds, Sheffield & York

eprints@whiterose.ac.uk
https://eprints.whiterose.ac.uk/

Testing microscopically derived descriptions of nuclear collectivity: Coulomb excitation of ^{22}Mg

J. Henderson[a,b], G. Hackman[a], P. Ruotsalainen[c], S. R. Stroberg[a,1], K. D. Launey[d], J. D. Holt[a], F. A. Ali[e,f],
N. Bernier[a,g], M. A. Bentley[h], M. Bowry[a], R. Caballero-Folch[a], L. J. Evitts[a,i], R. Frederick[a], A. B. Garnsworthy[a],
P. E. Garrett[f], B. Jigmeddorj[f], A. I. Kilic[f], J. Lassen[a], J. Measures[a,i], D. Muecher[f], B. Olaizola[a,f], E. O'Sullivan[a],
O. Paetkau[a], J. Park[a,g,2], J. Smallcombe[a], C. E. Svensson[f], R. Wadsworth[h], C. Y. Wu[b]

[a]*TRIUMF, Vancouver, BC V6T 2A3, Canada*
[b]*Lawrence Livermore National Laboratory, Livermore, CA 94550, USA*
[c]*Department of Physics, University of Jyväskylä, FIN-40014 Finland*
[d]*Department of Physics and Astronomy, Louisiana State University, Baton Rouge 70803 USA*
[e]*Department of Physics, College of Education, University of Sulaimani, P.O. Box 334, Sulaimani, Kurdistan Region, Iraq*
[f]*Department of Physics, University of Guelph, Guelph, ON N1G 2W1, Canada*
[g]*Department of Physics and Astronomy, University of British Columbia, Vancouver V6T 1Z1, Canada*
[h]*Department of Physics, University of York, Heslington, York, YO10 5DD, UK*
[i]*Department of Physics, University of Surrey, Guildford, GU2 7XH, United Kingdom*

Abstract

Many-body nuclear theory utilizing microscopic or chiral potentials has developed to the point that collectivity might be studied within a microscopic or *ab initio* framework without the use of effective charges; for example with the proper evolution of the $E2$ operator, or alternatively, through the use of an appropriate and manageable subset of particle-hole excitations. We present a precise determination of $E2$ strength in ^{22}Mg and its mirror ^{22}Ne by Coulomb excitation, allowing for rigorous comparisons with theory. No-core symplectic shell-model calculations were performed and agree with the new $B(E2)$ values while in-medium similarity-renormalization-group calculations consistently underpredict the absolute strength, with the missing strength found to have both isoscalar and isovector components. The discrepancy between two microscopic models demonstrates the sensitivity of $E2$ strength to the choice of many-body approximation employed.

Keywords: ^{22}Mg; ^{22}Ne; Ab initio; Collectivity; Coulomb excitation

1. Introduction

Recent developments in many-body nuclear theory have seen a great advance in the number of nuclei accessible to microscopically derived theoretical models - including those constructed in an *ab initio* framework [1–15]. As these models increasingly reach regions of the nuclear landscape inaccessible to experiment, it is essential that their performance is scrutinized in detail using less-exotic systems where high-precision experimental data are available. The *sd*-shell lies between the traditional shell-model proton and neutron magic numbers of 8 and 20 and is an ideal laboratory for testing new models. The region contains examples of many phenomena found across the nuclear landscape, ranging from α-clustering [16] and Borromean-nuclei [17], to shell evolution [18] and high degrees of collective deformation [19]. In particular, the *sd*-shell provides an excellent opportunity for investigations of collectivity through the probing of first-excited 2^+ states in mid-shell even-even nuclei, which are typically dominated by collective degrees of freedom. By probing transitions to such states in mirror nuclei, one is additionally sensitive to charge-dependent effects in the interaction.

Historically, the phenomenological shell model has proved a successful tool in the modeling of this mass region, with empirically fit interactions typically well-reproducing experimental data [20]. A particular limi-
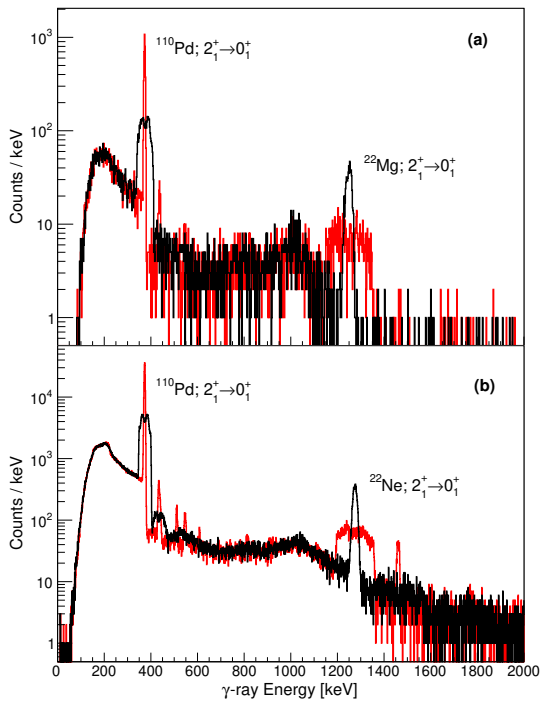
Figure 1: Doppler-corrected γ-ray spectra for (a) ^{22}Mg impinged on a ^{110}Pd target at 92.4 MeV, (b) ^{22}Ne impinged on a ^{110}Pd target at 54.8 MeV. Doppler-corrected for ^{22}Mg and ^{22}Ne (black) and ^{110}Pd (red).

Figure 2: Levels and transitions in ^{22}Mg (left) and ^{22}Ne (right) included in the Coulomb excitation analysis. Transitions for which matrix elements were varied in the χ^2 minimization are indicated by dashed arrows. Energy units are keV. Arrow widths correspond to relative branching ratios.

tation in the model, however, lies in the reproduction of nuclear collectivity - the bulk motion of many nucleons - and especially the electric-quadrupole ($E2$) strength commonly associated with it. As the shell model begins with an assumption of sphericity, collective $E2$ strength is generated through a coherent sum of many small-amplitude multi-particle multi-hole (mp-mh) excitations. A model space and interaction that achieve good reproduction of level energies does not necessarily reproduce transition strength. This strength is often underpredicted as the inclusion of a sufficiently large number of mp-mh excitations is in practice unfeasible. The typical approach is to explicitly compensate for this missing physics through an artificial inflation of the nucleon charges with phenomenological *effective charges*. It is therefore of considerable interest to determine whether modern microscopically derived nuclear theories are able to reproduce the experimentally observed collectivity in this region without the need for the phenomenologically derived corrections required in the shell model.

Accurate calculation of collective $E2$ strengths without the use of effective charges is currently being pur-
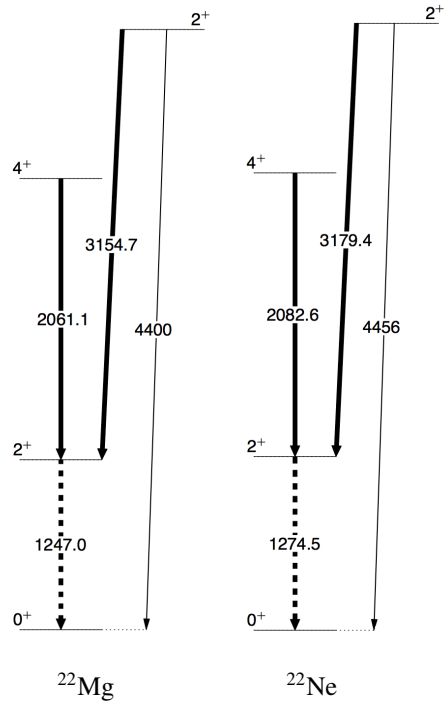
sued within several theoretical frameworks. For example, the no-core symplectic shell model (NCSpM) has in recent years determined $B(E2)$ values of nuclei within the *sd* shell, without resorting to such phenomenological corrections [21]. This model, though not strictly *ab initio*, provides the capability to reach large shell-model spaces using a microscopic interaction, while being in agreement with *ab initio* symmetry-adapted no-core shell-model [13] (SA-NCSM) calculations in smaller, more feasible model spaces that use the N2LO$_\text{opt}$ chiral potential [22]. A suite of *ab initio* many-body techniques are also able to perform calculations in the *sd*-shell with, for example, coupled-cluster (CC) [23], no-core shell model (NCSM) [24] and in-medium similarity-renormalization-group (IM-SRG) [25, 15] methodologies demonstrating promising results in terms of level-energy calculations. CC techniques reproduced transition strengths in self-conjugate ^{20}Ne and ^{24}Mg with precision comparable to the available experimental data [23]; however, this required the use of effective charges.

Two previous measurements of the 2^+_1 state lifetime in ^{22}Mg have been reported resulting in an evaluated $B(E2; 2^+_1 \rightarrow 0^+_1)$ of 95 ± 40 e^{2}fm^4 [26–28]. The sta-

ble nuclide ^{22}Ne has been well measured, with a precisely known lifetime yielding a $B(E2; 2_1^+ \rightarrow 0_1^+)$ value of 46.72 ± 0.66 e^{2}fm^4 [28]. Furthermore, the diagonal matrix element, $\langle 2_1^+ | E2 | 2_1^+ \rangle$, and thus the spectroscopic quadrupole moment of the 2_1^+ state, $Q_s(2_1^+)$ has also been measured in ^{22}Ne, yielding an evaluated value of $Q_s(2_1^+) = -0.19 \pm 0.04$ b [29]. In this Letter we present a Coulomb-excitation measurement of the $A = 22$ mirror pair, ^{22}Mg-^{22}Ne, through which we have significantly improved the precision of the ^{22}Mg $B(E2)$ and $Q_s(2^+)$ values. This represents the first measurement of $Q_s(2^+)$ in an even-even $T_z = \frac{1}{2}(N - Z) = -1$ nuclide, where Z (N) is the number of protons (neutrons). The new data are now of sufficient quality to test state-of-the-art microscopically derived theoretical calculations. It is found that NCSpM predictions for this $A = 22$ mirror pair are in excellent agreement with experimental transition strengths.

2. Experimental details

The first-excited 2^+ states in ^{22}Mg and its stable mirror ^{22}Ne were populated through Coulomb excitation in normal kinematics at the TRIUMF-ISAC-II facility. ^{22}Mg was produced using a 50 μA, 480-MeV proton beam impinged on a SiC target coupled to an ion guide laser ion source (IG-LIS) [30, 31]. With laser resonance ionization and suppression of isobaric contamination from surface ionization a ^{22}Na suppression in excess of 10^6 compared to the conventional hot cavity-laser ion source was achieved [32]. It was therefore possible to accelerate a clean beam of ^{22}Mg ions through the ISAC accelerator chain to the TIGRESS facility [33]. Two ^{22}Mg beam energies were used for the present measurement: 92.4 MeV and 83.4 MeV. Beam intensities at TIGRESS were maintained at approximately $1 \cdot 10^4$ pps throughout the experiment. The ^{22}Ne beam was provided by the offline ion-source (OLIS) and accelerated by the ISAC and ISAC-II accelerators to a final energy of 54.8 MeV with a mean intensity of approximately 5 ppA.

The ^{22}Mg (^{22}Ne) beam was impinged onto a 97.6-% enriched, 2.6-mg/cm^2 (1.6-mg/cm^2) thick ^{110}Pd target within the BAMBINO setup at the center of the TIGRESS array. For the present measurements BAMBINO consisted of a pair of Micron S3-type silicon detectors [34] covering angles of 20° to 49.4° and 131.6° to 160° in the laboratory frame. Scattered beam-like particles were detected in the BAMBINO S3 detectors and γ-rays de-exciting states populated in the beam- and target-like nuclei were detected with TIGRESS.

TIGRESS was operated in its high-efficiency configuration [35], with fourteen HPGe clover detectors at a target-to-detector distance of 11 cm. Data were acquired through the TIGRESS digital data acquisition system [36] using a single hit in one of the silicon detectors as the experimental trigger for the ^{22}Mg portion of the experiment, and with a particle-γ trigger for the higher-rate ^{22}Ne beam. A timing signal from the laser ion source was acquired with the experimental data and made it possible to distinguish prompt laser-ionized ^{22}Mg from time-random surface-ionized ^{22}Na events. This method of continuously monitoring surface ionized contamination was verified by periodically redirecting the beam into a Bragg detector [37] and yielded a ^{22}Na:^{22}Mg ratio over the course of the experiment of approximately 2%.

3. Analysis

Data were sorted using the in-house GRSISort [38] software package, built on the ROOT [39] data analysis framework. Particle-gated γ-ray spectra were Doppler corrected for beam-like and target-like scattering kinematics on an event-by-event basis, determined by the trajectory of the detected particle in the S3 detectors. Gamma-ray spectra, Doppler corrected for ^{22}Mg, ^{22}Ne and ^{110}Pd are shown in Fig. 1. Due to the higher beam energies used for the ^{22}Mg beams, the upstream S3 detector was excluded from the analysis as a result of lying in an "unsafe" Coulomb excitation regime, i.e. the distance of closest approach was less than 5 fm [40]. In the ^{22}Mg analysis the data were split into six angular bins, while the ^{22}Ne data were analyzed on a ring-by-ring basis to maximize sensitivity. The data were corrected for offsets in the x- and y-directions relative to the beam axis on the basis of asymmetries in the particle distributions on the S3 detectors. Addback was applied to the TIGRESS γ-ray spectra on the basis of the sub-crystal segmentation within the HPGe clover detectors. Gamma-ray detection efficiencies in TIGRESS were determined using ^{152}Eu, ^{133}Ba and ^{60}Co sources.

Efficiency-corrected ^{22}Mg, ^{22}Ne and ^{110}Pd Coulomb excitation yields were then evaluated using the GOSIA and GOSIA2 software packages [41], allowing for simultaneous analysis of both beam-like and target-like excitation. As described in Ref. [42], χ^2 surface distributions could thus be created for the $\langle 0^+ | E2 | 2^+ \rangle$ and $\langle 2^+ | E2 | 2^+ \rangle$ matrix elements in both ^{22}Ne and ^{22}Mg, based on excitation relative to the well-known low-lying matrix elements in ^{110}Pd which were included in the GOSIA analysis, with yields corrected to account for the
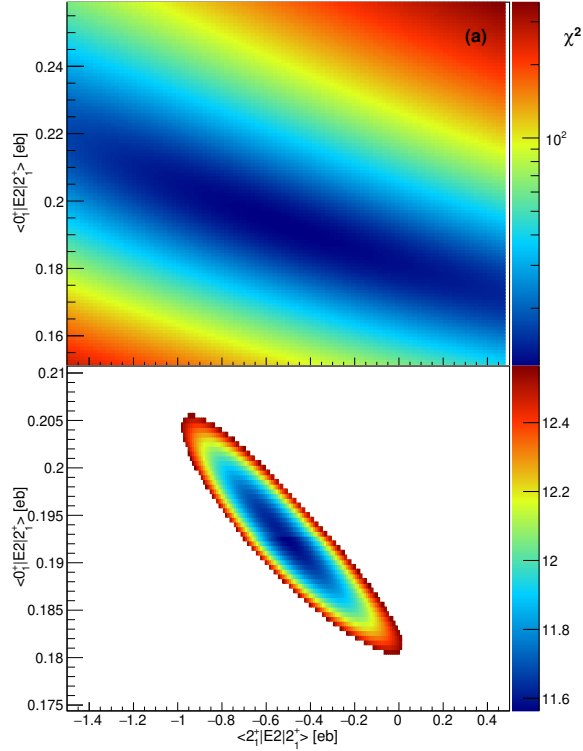
Figure 3: χ^2 surfaces in ^{22}Mg determined through a comparison of calculated Coulomb-excitation yields and experimental yields using GOSIA2 [41]. (a) Total χ^2 surface for the $\langle 0_1^+|E2|2_1^+\rangle$ and $\langle 2_1^+|E2|2_1^+\rangle$ matrix elements. (b) As (a) but within the $\chi^2_{min} + 1$ (1σ) limit, demonstrating the preference for a negative $\langle 2_1^+|E2|2_1^+\rangle$ matrix element.
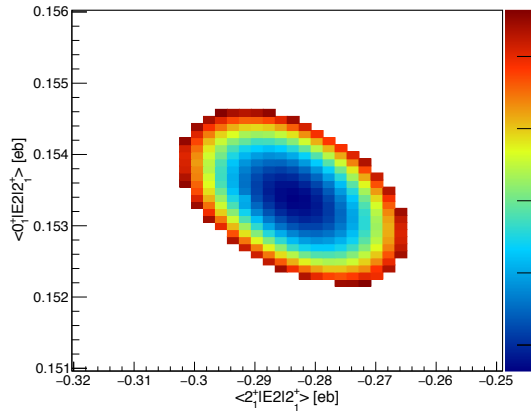

Figure 4: χ^2 surface at the $\chi^2_{min} + 1$ (1σ) limit for the $\langle 0_1^+|E2|2_1^+\rangle$ and $\langle 2_1^+|E2|2_1^+\rangle$ matrix elements in ^{22}Ne.

degree of enrichment of the target and the contamination in the beam. Literature $\langle 0_1^+|E2|2_1^+\rangle$ and $\langle 2_1^+|E2|2_1^+\rangle$ matrix elements for ^{22}Ne and ^{22}Mg were not included as experimental inputs in the analysis. The levels and transitions included in the analysis for ^{22}Ne and ^{22}Mg are shown in Fig. 2. Figures 3 and 4 show the total and 1σ χ^2 surface distributions plotted for ^{22}Mg, and the 1σ χ^2 surface for ^{22}Ne, respectively. Based on these analyses, values for the matrix elements were extracted and are summarized in Table 1 alongside literature values, where available, and theoretical values.

4. Discussion

The determined $B(E2; 2_1^+ \rightarrow 0_1^+)$ value in ^{22}Mg is approximately 20% lower than the evaluated value reported in the literature [28]. The present value lies within the 1σ uncertainties of the literature value but is considerably more precise. Taking a weighted average of the ^{22}Mg literature values [26, 27] and present values yields $B(E2; 2_1^+ \rightarrow 0_1^+) = 76.5^{+9.9}_{-7.4}$ e^{2}fm^4. Asymmetric uncertainties were combined using the method outlined in Ref. [44]. The extracted $\langle 2_1^+|E2|2_1^+\rangle$ matrix element is negative, indicating a preference for prolate deformation. The ^{22}Mg $B(E2; 2_1^+ \rightarrow 0_1^+)$ value now has uncertainties comparable to the other $T_z = -1$ nuclei, as shown in Fig. 5 in which the updated data are plotted with theory.

For ^{22}Ne good agreement is obtained with the well-known literature transition matrix elements, confirming the validity of the analysis. While agreeing at approximately the 2σ limit with the evaluated $\langle 2_1^+|E2|2_1^+\rangle$ value, the present result is in best agreement with the values obtained in Ref. [43]. The present $\langle 2_1^+|E2|2_1^+\rangle$ matrix element is more than a factor of two more precise than the evaluated values (see Tab. 1). Incorporating the present result a new weighted average value of $\langle 2_1^+|E2|2_1^+\rangle = -0.283 \pm 0.015$ eb is obtained, corresponding to $Q_s(2_1^+) = -0.215 \pm 0.011$ eb. Coupling the present result with the literature yields a new weighted average value of $B(E2; 2_1^+ \rightarrow 0_1^+) = 46.9 \pm 0.5$ e^{2}fm^4.

As shown in Fig. 5, the NCSpM reproduces the $A = 22, 26$ and 30 data well. NCSpM calculations are performed with a harmonic oscillator frequency, $\hbar\omega = 15$ MeV in a model space of 15 major shells. The calculations agree with *ab initio* SA-NCSM results using the N2LO$_{opt}$ where calculations are feasible [45] (e.g., for ^{22}Mg in 9 shells, $B(E2)$ strengths differ by 0.4%). We note that to achieve the converged $B(E2)$ values shown in Fig. 5, it is important to include mp-mh excitations to very high shells, as achieved in the NCSpM [46]. Allowing for the modest theoretical uncertainties resulting

	Shell model	IM-SRG		NCSpM	Experiment		
^{22}Ne	USDB	EM1.8/2.0	N$_2$LO$_{Opt}$		This Work	Literature	Ref.
$E(2^+)$ keV	1363	1657	1248	874		1274.54±0.01	[28]
$B(E2)$ e^{2}fm^4	48.97	20.0	18.5	50.8	47.06±0.62	46.72±0.66	[28]
$Q_s(2_1^+)$ eb	-0.139	-0.086	-0.096	-0.15	-0.215±0.012	-0.21±0.04	[43]
						-0.17±0.03	[28]
^{22}Mg							
$E(2^+)$ keV	1363	1604	1201	874		1247.02±0.03	[28]
$B(E2)$ e^{2}fm^4	65.8	41.3	35.5	73.2	$76.1\pm^{9.2}_{9.8}$	$95.2\pm^{62.4}_{26.8}$	[28]
						$268\pm^{201}_{183}$	[26]
						$64.6\pm^{34.2}_{16.6}$	[27]
$Q_s(2_1^+)$ eb	-0.16	-0.13	-0.13	-0.18	$-0.43\pm^{0.43}_{0.38}$		

Table 1: $B(E2)$ values and quadrupole moments for ^{22}Ne and ^{22}Mg as determined in the present work. Also shown are literature values, where available, including excitation energies. $B(E2)$ values correspond to $B(E2; 2_1^+ \to 0_1^+)$. Quoted uncertainties include systematic uncertainties arising from the beam composition analysis, the ^{110}Pd $B(E2)$, the target composition and the γ-ray detection efficiencies. Theoretical values are included for the shell-model, IM-SRG and NCSpM methodologies, with IM-SRG values shown for two interactions. Shell-model values were calculated using effective charges of $e^\pi = 1.36$ and $e^\nu = 0.45$.

from 5% variations in the model parameters shown in Fig. 5, the NCSpM provides excellent agreement with the experimental $B(E2)$ data for both $T_z = \pm 1$ nuclei.

Also shown in Fig. 5 are calculations performed using the valence-space IM-SRG formalism [47, 48, 25, 15] using a consistently evolved $E2$ operator (see Ref. [49] for details of the operator evolution) without incorporating effective charges. These calculations were performed *ab initio* using both the SRG-renormalized [50] 1.8/2.0 chiral interaction [51–53] and the N2LO$_{opt}$ interaction with a harmonic oscillator basis of $\hbar\omega = 20$ MeV, and with operators truncated at the two-body level. Clearly, these values significantly underpredict the $B(E2; 2_1^+ \to 0_1^+)$ strength. It should be noted, however, that the IM-SRG calculations do provide a good qualitative description of the $E2$ strength with increasing mass. Note that variations in the theoretical values for the excitation energies reflect differences in the fine details of the interactions used.

For comparison phenomenological shell-model calculations were performed using the USDB interaction using NuShellX [54] with some of the common combinations of effective charge [20, 54, 55]. The new data indicate that, while the phenomenological shell-model is able to reproduce the $A = 22$ case with a given choice of effective charge, no single combination of effective charges is able to reproduce the entire *sd*-shell, with notable deviations at $T_z = -1$, $A = 26$ and $T_z = +1$, $A = 34$.

The origin of the shortfall in $E2$ strength from the IM-SRG calculations is not yet fully understood, but must reside in the discarded terms involving three-body or higher-body operators. Work in this direction is currently in progress. The nature of the missing strength was assessed by normalizing the $B(E2)$ data according to the ratio of the theoretical and experimental values of the mirror partner. For example, a $B(E2)$ strength for the proton-rich mirror was projected as:

$$B(E2)_{T_z=-1}^{\text{Proj.}} = B(E2)_{T_z=-1}^{\text{Theory}} \times \frac{B(E2)_{T_z=+1}^{\text{Exp}}}{B(E2)_{T_z=+1}^{\text{Theory}}}, \quad (1)$$

This analysis was performed for both IM-SRG and shell-model calculations and the projected $B(E2)$ values were compared with experiment. It is found that, with the exception of mirror-pairs containing a magic number, the IM-SRG results are highly consistent, over-projecting the proton-rich strength by a factor of approximately 15% for the EM1.8/2.0 interaction. If the missing strength were purely isoscalar, a common scaling between theory and experiment would be expected for the $T_z = +1$ and $T_z = -1$ members of the mirror pair. The common 15% discrepancy therefore indicates that the missing strength is not purely isoscalar, and that a non-negligible isovector component must also be incorporated. Shell-model calculations - both with and without effective charges - on the other hand, exhibit no such consistent behavior in this analysis.
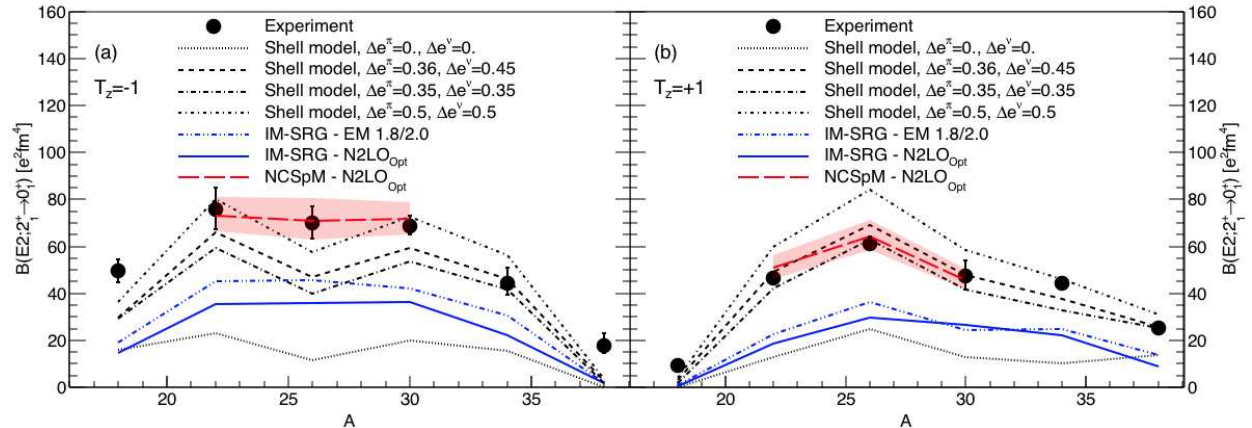
Figure 5: Experimental $B(E2; 2_1^+ \rightarrow 0_1^+)$ values for even-even, $T_z = -1$ (a) and $T_z = +1$ (b) mirror nuclei in the sd-shell, including the present value for ^{22}Mg. NCSpM calculations are shown for the $A = 22$, 26 and 30 mirror pairs and IM-SRG calculations are shown with an evolved effective $E2$ operator but with no further adjustment to the nucleon charges. IM-SRG calculations are shown for two interactions, N2LO$_{\text{Opt}}$ and EM1.8/2.0. Also shown are USDB shell model calculations for a number of common charge modifying combinations (Δe^π and Δe^ν modifying the proton and neutron charges, respectively). Finally, "bare" USDB shell model calculations are also shown, without adjustment to nucleon charges. The error band on the NCSpM values correspond to the spread in $B(E2)$ values arising from variations of 5% in the model parameters.

5. Conclusions

In conclusion, we present an improved measurement of the low-lying $E2$ strength in the $|T_z| = 1$, $A = 22$ mirror pair. A first Coulomb-excitation measurement of ^{22}Mg has been performed, indicating its prolate deformation at the first-excited $J^\pi = 2^+$ state and significantly improving the uncertainty of the $B(E2; 2_1^+ \rightarrow 0_1^+)$ value. This represents the first spectroscopic quadrupole moment measurement for an even-even $N < Z$ nuclide. Comparison with the state-of-the-art no-core symplectic shell model calculations, validated in smaller model spaces by the *ab initio* SA-NCSM, show excellent agreement in the $A = 22$, $A = 26$ and $A = 30$ cases without a reliance on effective charges. On the other hand, the valence-space IM-SRG, provides good qualitative agreement of the evolution of $E2$ strength, but dramatically underpredicts the absolute values. These agreements provide some promise for reaching descriptions of enhanced collectivity in sd-shell nuclei in the framework of the *ab initio* theory starting with chiral potentials. The failure of the IM-SRG to reproduce the data in contrast to the NCSpM demonstrates the sensitivity of $E2$ strength to the choice of many-body approximation employed, which needs to be further explored.

6. Acknowledgements

[1] E. Epelbaum, H.-W. Hammer, and U.-G. Meißner. *Rev. Mod. Phys.*, 81:1773, 2009.

[2] R. Machleidt and D.R. Entem. *Phys. Rep.*, 503:1, 2011.

[3] P. Navratil, S. Quaglioni, I. Stetcu, and B. R. Barrett. *J. Phys. G*, 36:083101, 2009.

[4] S. K. Bogner, R. J. Furnstahl, and A. Schwenk. *Prog. Part. Nucl. Phys.*, 65:94, 2010.

[5] K. Hebeler, J. D. Holt, J. Menéndez, and A. Schwenk. *Ann. Rev. Nucl. Part. Sci.*, 65:457, 2015.

[6] J. Carlson, S. Gandolfi, F. Pederiva, S. C. Pieper, R. Schiavilla, K. E. Schmidt, and R. B. Wiringa. *Rev. Mod. Phys.*, 87:1067, 2015.

[7] B.R. Barrett, P. Navrátil, and J.P. Vary. *Prog. Part. Nucl. Phys.*, 69:131, 2013.

[8] G. Hagen, T. Papenbrock, M. Hjorth-Jensen, and D.J. Dean. *Rep. Prog. Phys.*, 77:096302, 2014.

[9] W Dickhoff and C Barbieri. *Prog. Part. Nucl. Phys.*, 52:377, 2004.

[10] H. Hergert et al. *Phys. Rep.*, 621:165, 2016.

[11] E. Epelbaum, H. Krebs, D. Lee, and U.-G. Meissner. *Phys. Rev. Lett.*, 106:192501, 2011.

[12] S. Bacca, N. Barnea, W. Leidemann, and G. Orlandini. *Phys. Rev. Lett.*, 110:042503, 2013.

[13] K. D Launey, T. Dytrych, and J. P. Draayer. *Prog. Part. Nucl. Phys.*, 89:101, 2016.

[14] R. Roth and P. Navratil. *Phys. Rev. Lett.*, 99:092501, 2007.

[15] S. R. Stroberg et al. *Phys. Rev. Letts.*, 118:032502, 2017.

[16] Y. Chiba, M. Kimura, and Y. Taniguchi. *Phys. Rev. C*, 93:034319, 2016.

[17] T. Oishi, K. Hanino, and H. Sagawa. *Phys. Rev. C*, 82:024315, 2010.

[18] E. K. Warburton, J. A. Becker, and B. A Brown. *Phys. Rev. C*, 41:1147, 1990.

[19] N. Hinohara and Y. Kanada-En'yo. *Phys. Rev. C*, 83:014321, 2011.

[20] B. A. Brown and W. A. Richter. *Phys. Rev. C*, 74:034315, 2006.

[21] G. K. Tobin et al. *Phys. Rev. C*, 89:034312, 2014.

[22] A. Ekström et al. *Phys. Rev. Lett.*, 110:192502, 2013.

[23] G. R. Jansen et al. *Phys. Rev. C*, 94:011301R, 2016.

[24] E. Dikmen et al. *Phys. Rev. C*, 91:064301, 2015.

[25] S. R. Stroberg et al. *Phys. Rev. C.*, 93:051301(R), 2016.

[26] C. Rolfs. *Nucl. Phys. A*, 191:209, 1972.

[27] H. Grawe, K. Holzer, and K. Kändler. *Nucl. Phys. A*, 237:18, 1975.

[28] NNDC. Evaluated Nuclear Structure Data File (ENSDF).

[29] Stone. *Atomic Data and Nuclear Data Tables*, 90:75, 2005.

[30] M. Dombsky et al. *Hyperfine Interactions*, 225:17, 2014.

[31] P. G. Bricault et al. *Hyperfine Interactions*, 225:25, 2014.

[32] S. Raeder et al. *Rev. Sci. Inst.*, 85:033309, 2014.

[33] G. Hackman and C. E. Svensson. *Hyperfine Int.*, 225:241, 2014.

[34] Micron Semiconductor Ltd. Micron catalogue, 2017.

[35] C. E. Svensson et al. *J. Phys. G*, 31:1663, 2005.

[36] J. P. Martin, C. Mercier, N. Starinski, C. J. Pearson, and P. A Amaudruz. *IEEE Trans. Nucl. Sci*, 55:84, 2008.

[37] G. Hackman et al. *In Preparation*.

[38] Grsisort. https://github.com/GRIFFINCollaboration/GRSISort/.

[39] R. Brun and F. Rademakers. *Nucl. Instr. Meth. in Phys. Res. A*, 389:81, 1997.

[40] D. Cline. *Annu. Rev. Part. Nucl. Sci*, 36:683, 1986.

[41] T. Czosnyka, D. Cline, and C. Y. Wu. *Bull. Am. Phys. Soc.*, 28:745, 1983.

[42] M. Zielińska et al. *Eur. Phys. Jour. A*, 52:99, 2015.

[43] K. Nakai, F. S. Stephens, and R. M. Diamond. *Nucl. Phys. A*, 150:114, 1970.

[44] R Barlow. *arXiv:physics/0401042 Proceedings of the PHYS-TAT2003 conference*, 2003.

[45] G. Sargsyan. Private communication.

[46] A. C. Dreyfuss et al. *Physical Review C*, 95:044312, 2017.

[47] K. Tsukiyama et al. *Phys. Rev. C*, 85:061304, Jun 2012.

[48] S. K. Bogner et al. *Phys. Rev. Lett.*, 113:142501, 2014.

[49] N. M. Parzuchowski et al. *Phys. Rev. C*, 96:034324, 2017.

[50] S. K. Bogner et al. *Phys. Rev. C*, 75:061001(R), 2007.

[51] K. Hebeler et al. *Phys. Rev. C*, 83:031301R, 2011.

[52] J. Simonis et al. *Phys. Rev. C*, 93:011302(R), 2016.

[53] J. Simonis et al. *Phys. Rev. C*, 96:014303, 2017.

[54] B. A. Brown and W. D. M. Rae. *Nucl. Data Sheets*, 120:115, 2014.

[55] A. Wendt et al. *Phys. Rev. C*, 90:054301, 2014.